

A Handheld Device for Apple Ripeness and Sweetness Grading with Convolutional Neural Network

Shilpa Shailesh Gaikwad^{1*}, Sonali Kothari²

¹Electronics and Telecommunication Engineering, Symbiosis Institute of Technology, Symbiosis International (Deemed) University, Near Lupin Research Park, Gram-Lavale, Pune-412115, shilpa.gaikwad.phd2020@sitpune.edu.in, <https://orcid.org/0000-0002-2516-9238>

²Computer Science and Engineering, Symbiosis Institute of Technology, Symbiosis International (Deemed) University, Near Lupin Research Park, Gram-Lavale, Pune-412115, sonali.kothari@sitpune.edu.in, <https://orcid.org/0000-0002-3797-9932>

Abstract This research describes a handheld system developed for capturing multispectral images of apple fruit to evaluate quality based on ripeness and sweetness. The device consists of a 7-inch touchscreen display powered by a Raspberry Pi 5 and a rechargeable power bank, offering flexibility for field operation. A USB digital microscope camera with 1000× magnification is used to acquire detailed images. Multispectral data is captured using a Digitek lighting device, which provides sequential illumination in six color wavelengths: red, yellow, green, cyan, blue, and magenta. Image capture is automated through Python-based code that controls the lighting sequence and image acquisition. To grade apples by ripeness, a DenseNet-121 convolutional neural network was trained on the collected images, achieving an accuracy of 73.77%. For grading by sweetness, a multi-architecture approach, evaluating both custom convolutional neural networks (CNNs) and transfer learning models based on pre-trained VGG16, ResNet50, and EfficientNetB0 architectures fine-tuned on ImageNet weights was employed, reaching an accuracy of 66.22%. The results demonstrate the feasibility of using low-cost, handheld device paired with deep learning techniques for non-destructive fruit quality evaluation. The system holds promise for on-site grading in agricultural environments, reducing the dependence on hard-to-use and costly laboratory equipment.

Keywords: handheld device, grading, ripeness, sweetness.

1. INTRODUCTION

The evaluation of fruit quality is essential from a consumer and market perspective. Traditionally, human experts have evaluated fruit by visual inspection, which is often labor-intensive, time-consuming, and prone to inconsistencies [1]. Manual sorting cannot guarantee accuracy across large quantities, especially when internal attributes such as sweetness or ripeness are not visible. In recent years, the use of imaging techniques—particularly multi-spectral imaging—has enabled automation in fruit grading, helping to reduce labour costs while improving speed and consistency.

Fruit quality includes both external and internal characteristics. External factors such as color, size, shape, and surface defects are commonly used for initial grading [2]. Internal attributes like sweetness, acidity, firmness, and nutritional content play a critical role in determining the fruit's taste and market value [3]. Among these, ripeness and sweetness are two key indicators that directly affect consumer satisfaction. Accurate grading of these qualities not only helps sellers maintain quality standards but also reduces post-harvest losses and supports better cost.

Conventional methods used to examine internal quality are often destructive. In many cases, a fruit must be cut or pierced to measure sugar levels or determine ripeness. This leads to fruit loss, especially when used for large batch sampling. Some commercial tools such as the Wensar LMSP-V320 Spectrophotometer [4], Felix F-750 Produce Quality Meter [5], and NIRMagic Fruit Analyzer [6] use advanced spectral imaging for internal evaluation, but these devices are costly and not suitable for routine use by small-scale farmers or field workers. For instance, while the Felix F-750 offers rapid, non-destructive sugar analysis, its cost exceeds Rs. 7.5 lakhs, placing it out of reach for most users in low-resource settings. Additionally, such devices are often bulky, limiting their use to lab-based environments.

In contrast, non-invasive techniques such as multi-spectral imaging, combined with deep learning, provide a practical solution. Multi-spectral images are captured under different lighting wavelengths to reveal properties not visible under normal light. These images can be processed using deep learning methods,

especially Convolutional Neural Networks (CNNs), to classify fruit based on learned patterns. CNNs are especially useful in image-based classification tasks due to their ability to extract fine-grained spatial features, reduce manual feature engineering, and adapt to different types of image data. By using separate models for each task, such as DenseNet-121 for ripeness grading and a custom deep CNN for sweetness, the system can be optimized for higher accuracy over time.

This research introduces a low-cost, handheld device for grading apples based on ripeness and sweetness. The device is powered by a Raspberry Pi 5, includes a 7-inch touchscreen display for easy operation, and uses a USB micro scope camera with 1000× magnification. Six different color illuminations—red, yellow, green, cyan, blue, and magenta—are provided through a Digitek lighting device, and image capture is controlled through Python code. The system is lightweight, portable, and can be operated in field conditions without access to a lab. It enables users to collect image data and analyze it on-site using deep learning models trained on the same type of images. The device offers an affordable solution in the range of Rs. 20,000 to 25,000, making it a practical choice for small-scale fruit sellers, farmers, or researchers working in agricultural quality evaluation.

2. RELATED WORK

The non-destructive evaluation of fruit and vegetable quality is a critical area of research, aiming to reduce postharvest losses, ensure consumer satisfaction, and optimize supply chain logistics. Spectral imaging, encompassing both multispectral (MSI) and hyperspectral (HSI) techniques, has emerged as a powerful tool for this purpose. A review by Lorente et al. [7] established the foundational potential of HSI for evaluating a wide range of quality attributes, from ripeness and defects to chemical composition. However, a significant historical limitation was the reliance on bulky, expensive, and lab-based equipment, which hindered practical, in-field application. The subsequent literature demonstrates a clear and concerted effort to overcome this challenge by developing portable, low-cost, and user-friendly spectral imaging systems.

A main trend in the field is the development of custom-built, portable devices. Lopez Ruiz et al. [8] pioneered an early example with a portable MSI system based on a Raspberry Pi, demonstrating the feasibility of using affordable, off-the-shelf components. This concept was further refined by Noguera et al. [9], who developed a new, low-cost, hand-held multispectral device specifically for in-field fruit-ripening assessment, emphasizing practicality and accessibility. Similarly, Guo et al. [10] created a novel handheld detector for measuring soluble solids content (sweetness), and Singh et al. [11] designed an “ultra-low-cost” self-referencing multispectral detector, showcasing that cost reduction is a central goal. More complex systems, such as the portable 3CCD camera system by Lee et al. [12], also contributed to the miniaturization of high-quality imaging technology for biological samples.

The ubiquity of smartphones has catalyzed a new wave of innovation. Goel et al. [13] introduced “HyperCam”, a groundbreaking project that adapted HSI for ubiquitous computing applications, laying the groundwork for mobile integration. More recently, Stuart et al. [14] demonstrated a low-cost HSI method using a standard smartphone, and Sharma et al. [15] introduced “MobiSpectral”, a system explicitly designed to bring hyperspectral imaging to mobile devices. These efforts democratize the technology, moving it from the specialized lab to the everyday user.

As hardware has become more accessible, research has increasingly focused on tailored applications and the sophisticated algorithms needed to interpret the spectral data. For instance, mango maturity has been a popular target. Wendel et al. [16] used HSI on a ground-based mobile platform for maturity estimation, while J“odicke et al. [17] employed MSI to monitor quality during the mango drying process. A crucial aspect of this work is the data processing pipeline. Zhang et al. [18] addressed the practical challenge of translating complex HSI data into more manageable MSI systems, investigating the portability and stability of algorithms for defect detection. This highlights the necessary trade-off between the rich data of HSI and the speed and simplicity of MSI, especially for portable devices. More recently, the focus has shifted towards advanced machine learning and deep learning models. He et al. [19] developed a handheld device that not only used MSI but combined it with fluorescence imaging and a lightweight convolutional neural network (CNN) for the rapid detection of citrus Huanglongbing. This represents a significant step forward, integrating multiple data sources and modern AI techniques into a single, portable solution.

3. METHODOLOGY

3.1 Component requirement for Handheld Device

The components required for the Handheld Device are given in Table 1.

Table 1: Component list for the Handheld Device.

Sr. No.	Component Name	Cost (INR)
1	Official Raspberry Pi Touch Display 2	6731
2	Raspberry Pi 5 Model 8GB	8289
3	Pro-Range 3 in 1 1000X 8 LED USB Microscope Camera Endoscope with stand Type-C Electronic Magnifier	1599
4	SanDisk V30 Extreme Pro 128GB microSDXC Card with 200MB/s Read, 90MB/s Write	1599
5	Ambrane 45W Fast Charging Powerbank, 15000mAh, USB-C and USB-A, Powerlit 45	2499
6	DIGITEK(LED-D10WRGB) 10W Portable RGB LED Light, 3 Color Modes, 360° Rotation, 2500-9000K	1899
7	4 bolts (8mm width by 120mm length), 16 washers, and 16 nuts	140
8	Foam Wood	180
	Total Cost	22,491

These components are grouped together to form the Portable Handheld device.

3.2 Device Design.

The device developed for this study is a portable, handheld system designed to capture multispectral images of apple fruits as shown in Figure 1. It consists of a Raspberry Pi 5 single-board computer connected to a 7-inch touchscreen display for interactive control. A USB microscope camera with up to 1000x magnification is used to capture detailed images of the fruit surface.

For lighting, a Digitek device is used to illuminate the apple under different color conditions. The system supports image capture under six specific colors: Red, Yellow, Green, Cyan, Blue, and Magenta. The entire setup is powered using a rechargeable power bank, making it suitable for use in the field without the need for direct power supply. The compact and lightweight design allows the device to be held and operated manually without any supporting frame or tripod. Python scripts control the lighting sequence and image capture process, making the device simple to operate.



(a) The front view



(b) The rear view

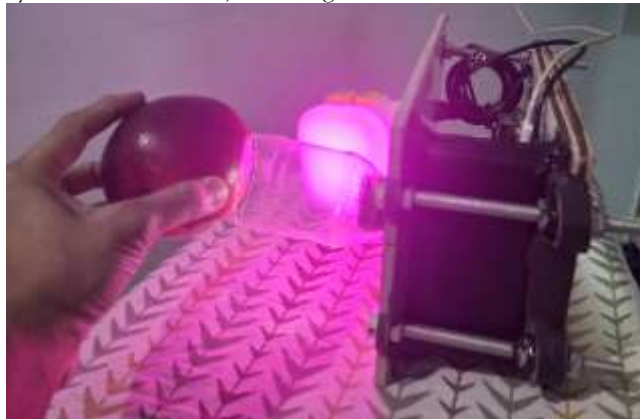
Figure 1. The Handheld Device.

3.3 Image Capture Process.

For each apple sample, a total of six multispectral images are captured—each under a different coloured light. The six colors used for illumination are Red, Yellow, Green, Cyan, Blue, and Magenta. The magenta illumination falling on the apple from the Digitek device is shown in Figure 2. These colors help in highlighting different surface features of the fruit that relate to its ripeness and sweetness. The lighting and image capture process is controlled using a Python script, which coordinates with the camera to capture an image under each lighting condition. However, the color selection on the Digitek light is done manually using two control knobs on the side of the device: The lower knob must be set to the HSI mode before capturing. The upper knob is a rotating dial, which sets the hue angle corresponding to the desired color:

- 0° for Red
- 60° for Yellow
- 120° for Green
- 180° for Cyan
- 240° for Blue
- 300° for Magenta

During image capture, the camera is kept at a fixed distance of approximately 7 cm from the apple. The system is handheld, allowing flexible use in natural environments.

**Figure 2.** The Handheld Device with Magenta illumination on the apple.**Figure 3.** The Concatenated Multi-Spectral image of Epli Apple.

3.4 Dataset Preparation

Apple Samples and Image Counts:

For ripeness grading, three apple varieties were used:

1. Red Delicious USA
2. Epli
3. Royal Gala

Each variety had 4 apples, observed over a period of 10 days. For each apple, 6 multispectral images were captured corresponding to six wavelengths (Red, Yellow, Green, Cyan, Blue, Magenta).

- Images per variety per day = 4 apples \times 6 wavelengths = 24 images
- For 3 varieties, images per day = 24 \times 3 = 72 images
- Over 10 days, total images = 72 \times 10 = 720 images

For sweetness grading, eight apple varieties were used:

1. Epli (label: epli)
2. Red Delicious USA (rdu)
3. Royal Gala (rg)
4. Granny Smith (gs)
5. Red Pop (redpop)
6. Washington USA (w)
7. Fuji (fuji)
8. Pink Lady (pl)

Each variety consisted of 4 apples, and 6 multispectral images were captured per apple, resulting in:

Total images = 8 varieties \times 4 apples \times 6 wavelengths = 192 image

Label Assignment

Labels were assigned according to apple variety codes as mentioned above, allowing classification by sweetness based on variety and ripeness over time.

Concatenation of the multi-spectral images

The multi-spectral images are concatenated with the help of the python code for all varieties of apple for grading by sweetness and ripeness and the concatenated image formed for Epli apple is shown in Figure 3.

Data Preprocessing

Images were preprocessed before training to improve model performance. For ripeness grading, images were preprocessed using the DenseNet121 input function which normalizes images accordingly. Data augmentation was applied during training but not directly in preprocessing. For sweetness grading, all input images underwent standardized preprocessing involving resizing to 224 \times 224 pixels using OpenCV's INTER_LINEAR interpolation, color space conversion from BGR to RGB format, and pixel intensity normalization to the range [0,1] through division by 255. To enhance model generalization and mitigate overfitting, comprehensive data augmentation was implemented using Keras Image DataGenerator with the following parameters: rotation range ($\pm 20^\circ$), width and height shifts ($\pm 20\%$), horizontal flipping enabled, while maintaining aspect ratio integrity. The augmentation pipeline was applied exclusively during training phases to preserve validation set authenticity.

Data Splitting

For ripeness grading, the dataset was split into 80% training and 20% validation sets. Similarly, the dataset was split into 75% training and 25% for the validation sets during sweetness grading to evaluate performance.

3.4 CNN Model for Ripeness Grading

For the ripeness grading, the DenseNet-121 architecture was used due to its ability to extract deep and meaningful features from images. The model was trained using a two-phase approach. In the first phase, only the classifier head was trained for 10 epochs. In the second phase, the entire model was fine-tuned for another 10 epochs to improve performance. The input images were resized and augmented using standard image augmentation techniques such as rotation, flipping, and zooming to increase data diversity and reduce overfitting. A batch size of 32 was used during training. The Adam optimizer was

chosen for its adaptive learning capabilities. The dataset was divided into training and validation sets in an 80:20 ratio. That is, 80% of the images were used for training, and 20% were used for validation. The DenseNet-121 model follows a deep feature extraction structure consisting of initial convolutional and pooling layers, followed by a series of dense blocks and transition layers, and a batch normalization layer before classification. The model achieved an accuracy of 73.77% in predicting the ripeness category of apples using multispectral images captured at six different color wavelengths.

3.5 CNN Model for Sweetness Grading

To classify apples by sweetness levels, a robust deep learning framework was developed utilizing Bayesian optimization for hyperparameter tuning across multiple neural network architectures. The classification system employed a multi-architecture approach, evaluating both custom convolutional neural networks (CNNs) with 2-4 convolutional blocks and transfer learning models based on pre-trained VGG16, ResNet50, and EfficientNetB0 architectures fine-tuned on ImageNet weights. Input images were standardized to 224×224 pixels with RGB color space normalization (pixel values scaled to 0-1 range), and data augmentation techniques including rotation ($\pm 20^\circ$), width/height shifts ($\pm 20\%$), and horizontal flipping were applied to enhance model generalization. The hyperparameter optimization process utilized Keras Tuner's Bayesian optimization with 30 maximum trials, systematically exploring optimizer selection (Adam vs. RMSprop), learning rates 10^{-5} to 10^{-3} , architectural parameters (filter sizes, dense units, dropout rates), and training configurations over 25 epochs per trial with early stopping patience of 5 epochs. The final model evaluation employed stratified train-validation splits (75:25 ratio) with performance evaluation including per-class precision, recall, and F1-score, confusion matrix evaluation, and prediction confidence distributions, ensuring robust validation of the five-class sweetness classification system (levels 10,11,12,13, and 14) with categorical cross entropy loss optimization.

The goal was to evaluate which architecture worked best for detecting subtle differences in multispectral images corresponding to varying sugar content in apples. The training setup was designed to be flexible for future improvements. Among all architectures evaluated, the custom CNN achieved the highest validation accuracy of 66.22%, outperforming the pre-trained VGG16, ResNet50, and EfficientNetB0 models in classifying sweetness levels.

Refractometer

A handheld refractometer is employed for manual measurement to evaluate the sweetness of each fruit in percentage Brix, and the fruits will be classified according to established grading methodologies [20]. First, cut the apple into 5 or 6 pieces and take the apple juice using a mixer. Then, sieve the apple juice with the help of Sieveer and pour it into a glass. Then, using a dropper, put one or two drops of the apple juice on the prism and close the flap. After this, hold the refractometer toward the light to read the apple sweetness through the eyepiece accurately.

The Lookup table for sugar content measurement of apples is shown in Table 2.

Table 2: Sugar Content Measurement of Apples in % Brix.

Sr. No.	Variety of Apple	Apple 1	Apple 2	Apple 3	Apple 4
1	Red Delicious USA	10	10	10	10
2	Epli	12	11	11	12
3	Royal Gala	11	10	11	13
4	Pink Lady	12	13	12	12
5	Red Pop	13	12	13	13
6	Washington	12	10	12	12
7	Granny Smith	10	11	10	10
8	Fuji	13	11	10	10

3.6 Model Architecture and Training

Ripeness Grading

For grading apples by ripeness, the DenseNet-121 convolutional neural network was used. The model was trained in two steps:

1. Initial Training: The classification head was trained for 10 epochs
2. Fine-Tuning: The full model was fine-tuned for an additional 10 epochs

Other training parameters included:

1. Batch Size: 32
2. Optimizer: Adam
3. Loss Function: Categorical Cross-entropy
4. Validation Split: 20% of data
5. Training Split: 80% of data

The architecture included key blocks such as:

1. Initial convolution and pooling layers (conv1, pool1)
2. Four dense blocks
3. Transition layers in between
4. Final classification layer with softmax activation

Data augmentation was included during training to improve model robustness.

Sweetness Grading

For sweetness classification, a deep learning approach with hyperparameter tuning was used. A tunable model was created with the following architecture options:

1. Custom CNN
2. Transfer Learning Models: VGG16, ResNet50, and EfficientNetB0

The models used pre-trained weights (ImageNet) with the classification head adapted for five sweetness classes: 10, 11, 12, 13, and 14.

The tuning process included:

1. Optimiser: Adam vs. RMSprop
2. Epochs per Trial: 25
3. Hyperparameter Trials: 30
4. Input Image Preprocessing: Resizing to 224×224 pixels using OpenCV's INTER_LINEAR interpolation, color space conversion from BGR to RGB format, and pixel intensity normalization to the range [0,1] through division by 255.

The model was trained using a custom Keras Tuner setup for optimal performance.

4. RESULTS

4.1 Grading by Ripeness

The ripeness classification model was evaluated using multiple metrics, including training and validation accuracy, loss, per-class performance, confusion matrix analysis, and timing breakdowns as shown in Figure 4. The overall classification achieved a final accuracy of 73.77% after a two-phase training procedure involving initial training and fine-tuning.

Accuracy and Loss Evaluation

As shown in the top left graphs of Figure 4, training and validation accuracy improved significantly after the fine-tuning phase, with validation accuracy rising from approximately 51.7% (initial training) to 73.8%. Correspondingly, the validation loss reduced from around 1.3 to 0.8, indicating better generalization after fine-tuning. The gap between training and validation metrics narrowed in later epochs, suggesting a reduction in overfitting.

Training Time and Speed

The total training time was 6073.69 seconds, with 1263.24 seconds spent on initial training and 4810.45 seconds on fine-tuning. Training time per epoch increased significantly during fine-tuning (Training Time per Epoch graph), leading to a shift in average training speed from approximately 6.5 images/sec to 3.5 images/sec (Training Speed graph). Fine-tuning accounted for 78.8% of total training time, as depicted in the time distribution pie chart.

Confusion Matrix and Class-wise Performance

The confusion matrix reveals that the model performed best on the "over-ripe" class, correctly classifying 149 instances, while under-ripe was more challenging, with noticeable confusion with the "ripe" class. Class-wise metrics (Precision, Recall, F1-Score) show that the model achieved the highest recall for the ripe class, while precision was strongest for over-ripe. The F1-score was relatively balanced across all classes, ranging from 0.70 to 0.76.

Overall Performance Metrics

The aggregated performance metrics indicate an accuracy of 0.738, precision of 0.757, recall of 0.738, and an F1-score of 0.731. These values affirm that the model is reasonably effective across all classes, with balanced precision and recall.

Prediction Time

Prediction efficiency was also evaluated. As shown in the "Prediction Time vs Batch Size" plot, prediction time increased linearly with batch size. The total time required for prediction on the test set was 28.84 seconds, corresponding to an average of 70.69 milliseconds per image.

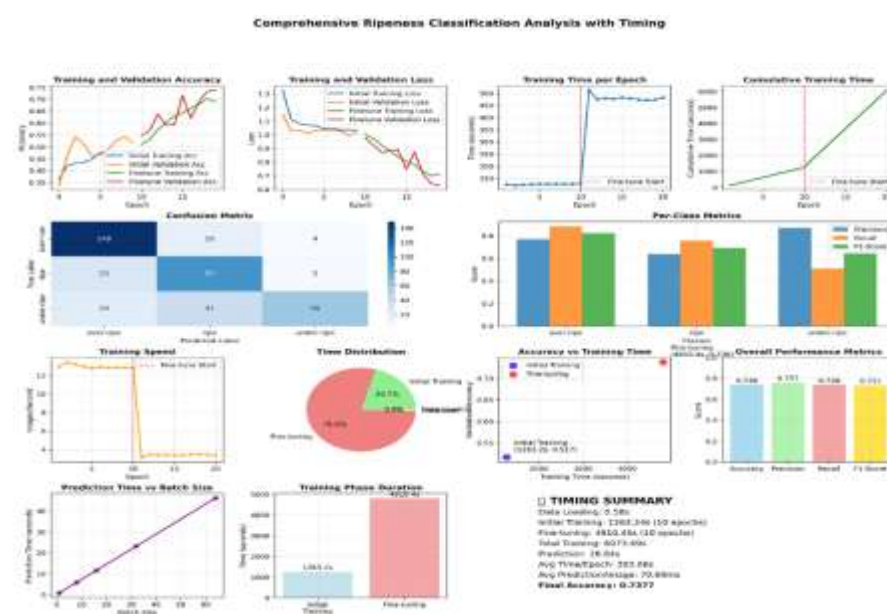


Figure 4. The Detailed Ripeness Classification Evaluation with Timing

4.2. Grading by Sweetness

The detailed model evaluation was conducted using multiple metrics, including accuracy, precision, recall, and F1-score, calculated for both overall performance and per-class metrics. Confusion matrices were generated for training and validation sets to evaluate classification patterns and identify potential class-specific weaknesses. Statistical significance was evaluated through stratified validation, while prediction confidence distributions were analyzed to evaluate model uncertainty quantification. Performance timing evaluation included total prediction time and per-image inference latency to evaluate computational efficiency.

Overall Performance Metrics

The trained model demonstrated robust performance across multiple metrics, achieving a validation accuracy of 66.22% with well-balanced precision (70.50%), F1-score (66%), and recall (66.22%).

Training Dynamics:

- Accuracy vs. Epoch: Shows convergence from ~ 25% to 65% with validation volatility indicating learning complexity.
- Loss vs. Epoch: Demonstrates consistent loss reduction from 1.6 to below 1.0, confirming effective optimization.
- Training Progress: Linear progression through 25 epochs showing systematic learning advancement.

Classification Performance:

- Training Confusion Matrix: Reveals strong diagonal patterns with Level 10 (54 correct) and Level 12 (41 correct) showing excellent classification.
- Validation Confusion Matrix: Shows balanced performance across classes with Level 10 (16 correct) and Level 12 (11 correct) maintaining consistency.
- Key Insight: Most errors occur between adjacent sweetness levels (e.g., The mappings are $10 \leftrightarrow 11$ and $12 \leftrightarrow 13$, which is expected and reasonable.



Figure 5. The Detailed Sweetness Classification Evaluation

Detailed Metrics Evaluation

- Per-Class Metrics: Level 14 achieves perfect precision (100%) but lower recall, while Level 10 shows strong recall (84%).
- Overall Metrics Comparison: Training and validation metrics are well-aligned (both ~66-70%), indicating good generalization without overfitting.
- Balanced Performance: Precision, recall, and F1-scores are consistently around 66.70% across both sets.

Data Insights and Model Behaviour Evaluation

- Class Distribution: Both training and validation sets show balanced representation across sweetness levels.
- Prediction Confidence: Bimodal distribution with peaks at 0.5 and 0.9 suggests the model makes both confident and uncertain predictions appropriately.
- Performance Summary: Final validation accuracy of 66.22% with 294 total images and 3.45s prediction time.

The dashboard reveals a well-trained model that successfully learned to distinguish apple sweetness levels with reasonable accuracy. The 66% validation accuracy represents strong performance for a 5-class visual classification, especially considering the subtle visual differences between sweetness levels. The balanced metrics across training and validation sets confirm robust generalization capability.'

5. CONCLUSIONS

This study demonstrates an effective deep learning-based approach for grading apple ripeness into overripe, ripe, and underripe categories using multispectral images. The results demonstrate that the model achieved a final accuracy of 73.77%, with notable improvements during the fine-tuning phase. Performance metrics, including precision (0.757), recall (0.738), and F1-score (0.731), confirm the model's

balanced predictive capability across all three ripeness levels. Analysis of the confusion matrix revealed that ripe and overripe classes were better identified compared to underripe, suggesting a need for more representative training samples or feature enhancement for underripe detection. Training and validation curves showed clear improvement across epochs, with fine-tuning substantially enhancing the model's generalization ability. Timing analysis indicated that fine-tuning constituted the majority of training time (over 78%), which contributed positively to performance gains. Additionally, the model maintained efficient prediction speeds, with an average inference time of 70.69 ms per image, supporting its suitability for real-time applications. Overall, the model offers a promising solution for automated, non-destructive ripeness assessment in agricultural contexts. Future work could explore advanced augmentation strategies, optimized class balancing, and lightweight architectures to further enhance accuracy while maintaining low computational overhead. In addition, this study also demonstrates a deep learning-based approach for classifying apples according to sweetness levels ranging from 10 to 14, using multispectral image data. The proposed model achieved a validation accuracy of 66.22% with a corresponding F1-score of 0.6600, precision of 0.7050, and recall of 0.6622, suggesting moderate but consistent classification performance across all sweetness levels.

The model exhibited particularly strong performance in classifying extreme sweetness levels, with Level 14 achieving near-perfect precision (100%) and Level 10 showing excellent recall (84%), suggesting the model successfully learned to distinguish between distinct sweetness categories. The confusion matrices reveal that classification errors primarily occurred between adjacent sweetness levels, which is expected given the inherent similarity between neighbouring categories and represents reasonable model behaviour. The balanced class distribution in both training (25.9% Level 10, 26.8% Level 12) and validation sets (25.7% Level 10, 27.0% Level 12) ensured fair evaluation across all sweetness levels, while the prediction confidence distribution shows the model's ability to make confident predictions with peaks around 0.5 and 0.9 probability ranges, indicating appropriate uncertainty quantification in its decision-making process. Despite these challenges, the model's ability to distinguish between fine sweetness levels in apples without invasive methods makes it a valuable tool for post-harvest quality sorting. Future enhancements could involve dataset balancing, integration of spectral feature selection, and model fusion to improve classification robustness and generalizability.

Acknowledgment: The authors would like to express their gratitude to Symbiosis International (Deemed) University, Pune for providing the necessary facilities and resources to conduct this research.

Credit Authorship contribution statement: Conceptualization: Shilpa Shailesh Gaikwad, Sonali Kothari; Methodology: Shilpa Shailesh Gaikwad; Formal analysis and investigation: Shilpa Shailesh Gaikwad; Writing – original draft preparation: Shilpa Shailesh Gaikwad; Writing – review and editing: Sonali Kothari; Funding acquisition: Shilpa Shailesh Gaikwad; Resources: Shilpa Shailesh Gaikwad; Supervision: Sonali Kothari. Both authors have read and approved the final manuscript.

Declaration of competing interest: The authors declare that there is no conflict of interest in the paper.

REFERENCES

- [1] Shilpa Gaikwad and Sonali Tidke. Multi-spectral imaging for fruits and vegetables. In *International Journal of Advanced Computer Science and Applications*, 13(2):743–760, 2022. doi:10.14569/IJACSA.2022.0130287.
- [2] Natalia Hernandez-Sanchez, Guillermo P Moreda, Ana Herre-ro Langreo, and Angela Melado-Herreros. Assessment of internal and external quality of fruits and vegetables. In *Imaging technologies and data processing for food engineers*, pages 269–309. Springer, 2016. doi:10.1007/978-3-319-24735-9_9.
- [3] S. Musacchi and S. Serra, "Apple fruit quality: Overview on pre-harvest factors," *Scientia Horticulturae*, vol. 234, pp. 409–430, 2018.
- [4] Wensar. v320, Wensar 2024. single beam URL spectrophotometer, lmsp <https://www.moglix.com/wensar-single-beam-spectrophotometer-lmsp-v320/mp/msno5wnn26pl51>. Accessed: 25 March 2025.
- [5] Felix Instruments. F-750 produce quality meter. <https://felixinstruments.com/food-science-instruments/nir-spectroscopy/f-750-produce-quality-meter/>. Accessed: 25 March 2025.
- [6] Instruments analyzer. Trade. Nirmagic1100 portable fruit near infrared <https://www.instrumentstrade.com/nirmagic1100-portable-fruit-near-infrared-analyzer>. Accessed: 25 March 2025.
- [7] Lorente, D., Aleixos, N., Gómez-Sanchis, J., Cubero, S., García-Navarrete, O.L., Blasco, J.: Recent advances and applications of hyperspectral imaging for fruit and vegetable quality assessment. *Food and Bioprocess Technology* 5(4), 1121–1142 (2012). doi:10.1007/s11947-011-0725-1.

- [8] Lopez-Ruiz, N., Granados-Ortega, F., Carvajal, M.A., Martinez-Olmos, A.: Portable multispectral imaging system based on raspberry pi. *Sensor Review* 37(3), 322–329 (2017). doi:10.1108/SR-12-2016-0276.
- [9] Noguera, M., Millan, B., Andújar, J.M.: New, low-cost, hand-held multispectral device for in-field fruit-ripening assessment. *Agriculture* 13(1), 4 (2022). doi:10.3390/agriculture13010004.
- [10] Guo, W., Li, W., Yang, B., Zhu, Z., Liu, D., Zhu, X.: A novel noninvasive and cost-effective handheld detector on soluble solids content of fruits. *Journal of food engineering* 257, 1–9 (2019). doi: 10.1016/j.jfoodeng.2019.03.022.
- [11] Singh, H., Sridhar, A., Saini, S.S.: Ultra-low-cost self-referencing multispectral detector for non-destructive measurement of fruit quality. *Food Analytical Methods* 13(10), 1879–1893 (2020). Doi:10.1007/s12161-020-01810-7.
- [12] Lee, H., Park, S.H., Noh, S.H., Lim, J., Kim, M.S.: Development of a portable 3ccd camera system for multispectral imaging of biological samples. *Sensors* 14(11), 20262–20273 (2014)
- [13] Goel, M., Whitmire, E., Mariakakis, A., Saponas, T.S., Joshi, N., Morris, D., Guenter, B., Gavrilu, M., Borriello, G., Patel, S.N.: Hypercam: hyperspectral imaging for ubiquitous computing applications. In: *Proceedings of the 2015 ACM International Joint Conference on Pervasive and Ubiquitous Computing*, pp. 145–156 (2015). doi:10.1145/2750858.280428.
- [14] Stuart, M.B., McGonigle, A.J., Davies, M., Hobbs, M.J., Boone, N.A., Stanger, L.R., Zhu, C., Pering, T.D., Willmott, J.R.: Low-cost hyperspectral imaging with a smartphone. *Journal of imaging* 7(8), 136 (2021).
- [15] Sharma, N., Waseem, M.S., Mirzaei, S., Hefeeda, M.: Mobispectral: Hyperspectral imaging on mobile devices. In: *Proceedings of the 29th Annual International Conference on Mobile Computing and Networking*, pp. 1–15 (2023).doi:10.1145/3570361.3613296.
- [16] Wendel, A., Underwood, J., Walsh, K.: Maturity estimation of mangoes using hyper spectral imaging from a ground based mobile platform. *Computers and Electronics in Agriculture* 155, 298–313 (2018). doi: 10.1016/j.compag.2018.10.021.
- [17] Jödicke, K., Zirkler, R., Eckhard, T., Hofacker, W., Jödicke, B.: High end quality measuring in mango drying through multi-spectral imaging systems. *ChemEngineering* 4(1), 8 (2020). Doi:10.3390/chemengineering4010008.
- [18] Zhang, B., Liu, L., Gu, B., Zhou, J., Huang, J., Tian, G.: From hyperspectral imaging to multispectral imaging: Portability and stability of his-mis algorithms for common defect detection. *Postharvest Biology and Technology* 137, 95–105 (2018). .doi:10.1016/j.postharvbio.2017.11.004.
- [19] He, C., Li, X., Liu, Y., Yang, B., Wu, Z., Tan, S., Ye, D., Weng, H.: Combining multicolor fluorescence imaging with multispectral reflectance imaging for rapid citrus huanglongbing detection based on lightweight convolutional neural network using a handheld device. *Computers and Electronics in Agriculture* 194, 106808 (2022). doi: 10.1016/j.compag.2022.106808.
- [20] Gaikwad, S., & Kothari, S. (2025). Deep learning framework for precision grading and non-invasive Apple sweetness evaluation. *International Journal on Smart Sensing and Intelligent Systems*, 18(1). <https://doi.org/10.2478/ijssis-2025-0007>